Effect of Human Presence on UWB Radiowave Propagation within the Passenger Cabin of a Midsize Airliner

Simon Chiu and David G. Michelson, *Senior Member, IEEE*

***Abstract*—We have characterized the effect of human presence on path gain and time dispersion over ultrawideband (UWB) channels within the passenger cabin of a typical midsize airliner. We measured a few hundred channel frequency responses over the range 3.1 – 6.1 GHz between various locations within a Boeing 737-200 aircraft, with and without volunteers occupying the passenger seats. The links were deployed in a point-to-multipoint configuration with the transmitting antenna along the centre-line of the forward part of the cabin at either the ceiling or headrest level and the receiving antenna at the headrest or armrest level at selected locations throughout the rest of the cabin. As the density of occupancy increased from empty to full, path gain dropped by no more than a few dB on the ceiling-to-headrest paths but dropped by up to 10 dB on the ceiling-to-armrest and headrest-to-armrest paths. The gain reduction reached its maximum at the mid-point of the cabin and decreased thereafter. In all cases, increasing the density of occupancy caused the distance dependence of the rms delay spread to decrease greatly, the decay rate of the scattered components in the power delay profile (PDP) to almost double and the number of significant paths to drop by almost half. The results suggest that human presence substantially affects both path gain and time dispersion within the aircraft and should therefore be considered when assessing the performance of in-cabin wireless systems.**

I. INTRODUCTION

HUMAN presence in the vicinity of a short-range, low-power wireless link often leads to shadowing and scattering that affect both the path gain and time dispersion experienced by the link [1],[2]. Concern for the effect of human presence on short-range wireless links has motivated both measurement- and simulation-based studies of: (1) the depth and duration of shadow fading due to pedestrians moving in the vicinity of such links [3]-[5], (2) the effect of human presence on wireless personal area networks (WPANs), *i.e.*, where one end of the link is located either close to or on a person [6]-[9], and (3) the effect of human presence on wireless body area networks (WBANs), *i.e.*, where both ends of the link are located either close to or on a person [10]-[12].

In recent years, airlines and aircraft manufacturers have expressed much interest in deploying short-range wireless links within the passenger cabins of airliners in order to: (1) permit deployment of in-flight entertainment (IFE) and network access services and (2) facilitate operations and maintenance through deployment of sensor networks [13]-[17]. Although various wireless technologies have been considered and evaluated, ultrawideband (UWB) wireless technology that operates within the frequency band between 3.1 and 10.6 GHz have attracted particular interest for future systems because it: (1) can support very high data rates (up to 480 Mbps) over short distances, (2) occupies a particularly small footprint, radiates little RF energy, and consumes little power, and (3) can support precise positioning capabilities.

With its cylindrical structure, its confined volume, the regular layout of its seating, and its high density of occupancy, an airliner passenger cabin is fundamentally different from the residential, commercial and industrial indoor environments considered previously by UWB researchers [18],[19]. The confined volume and high density of occupancy suggest that human presence will affect the performance of wireless systems in aircraft passenger cabins more than it will in other environments. Two previous studies presented characterizations of the UWB wireless channel within aircraft passenger cabins [20],[21], but disclosed only limited information concerning the effect of human presence on UWB wireless propagation in such environments. In other previous work, assessments of the excess pathloss introduced by human presence and internal components in passenger cabins were presented based upon: (1) narrowband measurements collected using CDMA handsets onboard a Boeing MD-90 with up to 17 passengers in the cabin [22] and (2) simulations of the effect of passengers and internal components on electromagnetic field strength inside Boeing B747, B767 and B777 aircraft passenger cabins [23]. Other previous work has yielded estimates of the manner in which the presence of windows, people and furnishings affect the field statistics and

Manuscript received April 16, 2009; revised July 28, 2009; accepted September 7, 2009.

S. Chiu and D.G. Michelson are with the Radio Science Laboratory, Department of Electrical and Computer Engineering, University of British Columbia, Vancouver, BC, Canada V6T 1Z4. Corresponding author: D. G. Michelson, tel: 604 822-3544, fax: 604 822-5949, email: davem@ece.ubc.ca.

This work was supported in part by grants from Nokia Products, Bell Canada (through its Bell University Labs program), and Western Economic Diversification Canada. It was conducted under certificates of approval issued by the Research Ethics Boards at the University of British Columbia and the British Columbia Institute of Technology.

spoil the Q-factor of an enclosed space that functions as a multimode cavity [25]. However, designers require a more complete description of the effect of human presence on propagation in aircraft passenger cabins that account for the different types of paths within such environments and which are based upon larger data sets. A very recent study, conducted about the same time, as ours, considered the effect of human presence on UWB propagation within a large wide-body aircraft [26]. Here, we present the results of a complementary study conducted within a smaller narrow-body aircraft.

After completing a pair of rigorous research ethics reviews and recruiting almost 100 volunteers to occupy passenger seats, we collected a few hundred UWB channel frequency responses (CFRs) over the frequency range of 3.1-6.1 GHz in a point-to-multipoint configuration within the passenger cabin of a Boeing 737-200 aircraft. We mounted the transmitting antenna at either the cabin ceiling or headrest level along the centerline of the forward part of the cabin and collected channel frequency response data with the receiving antenna mounted at headrest or armrest level at selected locations throughout the cabin with three degrees of occupancy: empty, partially filled and completely filled. We processed the result to determine the manner in which human presence affects the distance and frequency dependence of path gain, the form of the channel impulse response, the distance and frequency dependence of rms delay spread, and the number of significant paths below a given threshold within the passenger cabin of a typical mid-size airliner. We selected the frequency range 3.1-6.1 GHz, which corresponds closely to Band Groups 1 and 2 as defined by the WiMedia Alliance, because it is more likely that the lower portion of the UWB band will be used for point-to-multipoint coverage over large portions of the aircraft passenger cabin while the higher portions of the band are used to implement short-range peer-to-peer links [27].

The remainder of this paper is organized as follows. In Section II, we describe our VNA-based UWB channel sounder, our procedure for calibrating it, our data collection procedure and our measurement database. In Section III, we present the results of our investigation of path gain. In Section IV, we present the results of our investigation of time dispersion. Finally, in Section V, we summarize our key findings and their implications.

II. MEASUREMENT SETUP

A. UWB Channel Sounder

Our UWB channel sounder consists of an Agilent E8362B vector network analyzer (VNA), 4-m FLL-400 SuperFlex and 15-m LMR-400 UltraFlex coaxial cables, a pair of Electro-metrics 6865 omnidirectional UWB biconical antennas, tripods and fixtures suitable for mounting the antennas at various locations throughout the aircraft, and a laptop-based instrument controller equipped with a GPIB interface. During data collection, a MATLAB script running on the laptop controlled the VNA and logged the received data.

We recruited volunteers to occupy passenger seats during the measurement session. In order to meet RF emission limits imposed upon us by the Research Ethics Boards at the University of British Columbia and the British Columbia Institute of Technology, we set the transmit power to 5 dBm. We set the intermediate frequency bandwidth of the VNA to 3 kHz which reduced the resulting displayed average noise level (DANL) to -107.2 dBm. The minimum sweep time was automatically set to 2 seconds. As configured, the channel sounder can resolve channel impulse responses (CIRs) with an SNR $\geq$ 25 dB at transmitter-receiver separation distances of up to 15 m assuming a distance exponent of 2.2, based on the worst case observed in our previous work [20], and average transmit and receive antenna gains of 0 dBi over all angles and directions.

During data collection, the VNA was configured to sweep from 3.1 to 6.1 GHz over 2560 frequency points. The frequency sampling interval of 1.1718 MHz corresponds to a maximum unambiguous excess delay of 853 ns or a maximum observable distance of 256 m. The frequency span of 3 GHz gives us a temporal resolution of 333 ps or a spatial resolution of 100 mm.

B. Channel Sounder Calibration

Before measurement data can be collected, the channel sounder must be calibrated so that systematic variations in the amplitude and phase of the measured frequency response due to factors other than the propagation channel can be removed. The process involves two steps. The first step is to use the VNA's built-in calibration routines, which are based upon a standard 12-term error model, to compensate for amplitude and phase distortions up to the point where the cables attach to the transmitting and receiving antennas. Care must be taken to ensure that the distortions for which the error correction model is compensating do not change appreciably during the measurement session, *e.g.*, due to significant cable flexion and torsion, so that the error correction process will not introduce its own distortions. Appropriate cable handling and management techniques are the most effective way to avoid such problems.

The second step, which is much more difficult, is to compensate for the distortions introduced by the antennas themselves. Because the radiation patterns of practical UWB antennas vary with both direction and frequency, individual multipath components (MPCs) arriving at the receiving antenna from different directions will be distorted in different ways. The measured channel response includes elements of the response of both: (1) the propagation channel and (2) the transmitting and receiving antennas. The result is often referred to as the response of the radio channel. In order to perfectly de-embed the propagation channel response from the radio channel response, one would need to measure the frequency-dependent double-directional channel response that accounts for the angle-of-departure (AoD) and angle-of-arrival (AoA) of each ray and the frequency-dependent three-dimensional radiation pattern of each antenna [28].

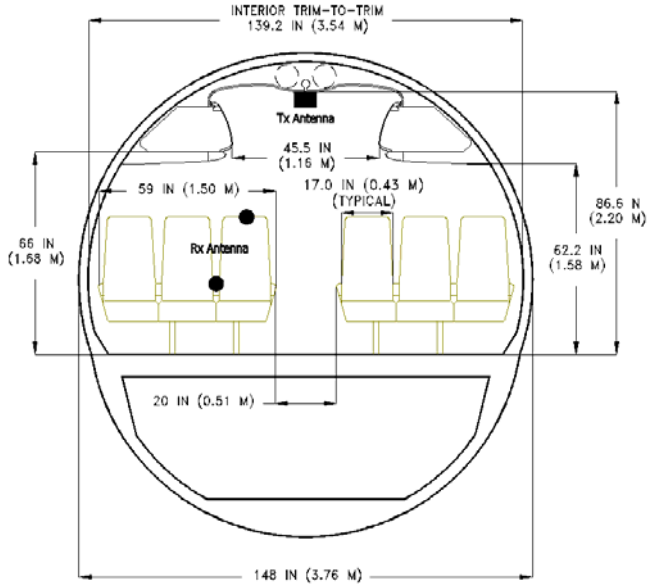

Fig. 1. Cross-sectional view of the passenger cabin showing the positions at which the transmitting and receiving antennas were deployed in the ceiling-to-headrest and ceiling-to-armrest configurations. The transmitting antenna is lowered to headrest level for the headrest-to-armrest configuration.

Implementing the required measurement setup within the confines of the aircraft passenger cabin would be problematic, however.

The antenna calibration problem is simplified considerably if we can assume that the environment is rich with scatterers so that the physical MPCs arrive from all possible directions and each resolvable MPC includes many physical MPCs. Because the directivity of any antenna averaged over all directions is unity for all frequencies, the measured CFR will be independent of the radiation patterns of the transmitting and receiving antennas. In such cases, after appropriate account has been taken for the return loss of the antennas and the amplitude of any line-of-sight (LOS) components, the measured channel response will be equivalent to the propagation channel response.

The dense single cluster form of the CIRs that we observed within that environment suggests that the density of scatterers within the cabin is very high. Moreover, previous work in conventional indoor environments has shown that the AoA distribution in the vertical plane broadens considerably as the size of the enclosed space becomes smaller [29]. Accordingly, it is not unreasonable to assume that the scattering is sufficiently broad that the effective gain of the transmitting and receiving antennas over all directions and frequencies is unity. Thus, while our results strictly characterize the *radio channel*, it seems likely that the measured channel is a useful approximation to the *propagation channel*.

C. Data Collection

We collected the CFR measurements within the passenger cabin of a Boeing 737-200 aircraft. The cabin, which can seat 130 passengers, is 3.54 m in width, 2.2 m in height and 21 m in length of which 18 m actually includes passenger seating. So that we could assess the effect of human presence on RF propagation aboard the passenger cabin, we collected measurement data with three levels of occupancy: empty, partially full and completely full. When the cabin was partially full, volunteer passengers sat in alternating seats from rows 4 through 19. When the cabin was full, volunteer passengers sat in every seat from row 4 through 19. During data collection, all of the passengers were asked to engage in quiet activities such as talking or reading while seated rather than standing in the aisle or moving about the aircraft. Before we collected production data, we verified that we could exploit the bilateral and translational symmetry inherent in the cabin layout to dramatically reduce the number of measurements needed to characterize propagation within the aircraft.

We mounted the transmitting antenna along the centerline of the cabin at row 2 at either ceiling or headrest height, as appropriate, in the manner of an access point. We considered three different path types: ceiling-to-headrest (C-to-H), ceiling-to-armrest (C-to-A) and headrest-to-armrest (H-to-A). For both the C-to-H and C-to-A path types, we mounted the transmitting antenna at the ceiling level and used a custom-designed mount to place the receiving antenna at the headrest or armrest level of passenger seats in a reproducible manner on the port side of the aircraft from rows 4 to 19. For the C-to-H path type, the receiving antenna was placed on alternating aisle, middle and window seats, while for the C-to-A path type, the receiving antenna was placed only on alternating middle and window seats. For the H-to-A path type, we mounted the transmitting antenna at the headrest level and placed the receiving antenna at the armrest level of alternating middle seats on the port side of the aircraft from rows 4 to 18. The two different receiving antenna mounting positions not only represent typical use cases such as using a cell phone (at headrest level) or a laptop (at armrest level) but also represent both LOS (at the headrest) and NLOS (at the armrest) channels. A cross-section view of the cabin that shows the various antenna mounting positions is given in Fig. 1. A plan view of the cabin is shown in Fig. 2.

D. Measurement Database

During the development phase, we considered three transmitter locations at rows 2, 11 and 16 and over 50 receiver locations in the empty passenger cabin. For selected paths, we took multiple sweeps to verify the static nature of the channel and the reproducibility of our measurements. This yielded over 200 CFRs in the development phase. During the production phase, we used only one transmitter location and collected data only on the port side of the aircraft. For each of the three levels of occupancy, *i.e.*, empty, partially filled and completely filled, we collected CFRs at 24 and 16 different receiver locations along the port side of the aircraft for the C-to-H and C-to-A path types, respectively. For the empty and full aircraft cases, we also collected CFRs at 8 selected receiver locations for the H-to-A path type. This yielded 152 CFRs in the production phase. In total, we collected over 360 CFRs.

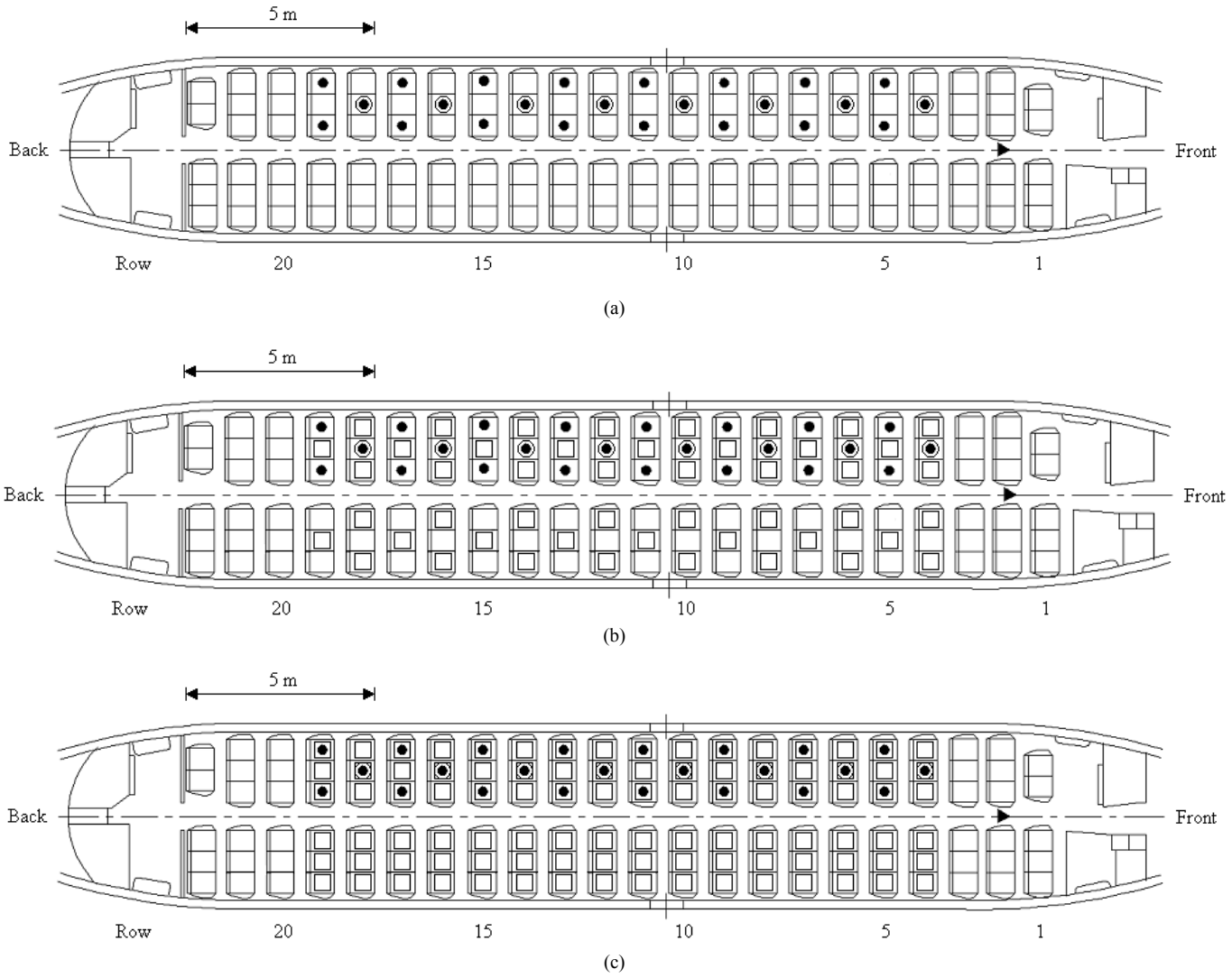

Fig. 2. Locations of the transmitting antenna (►), receiving antenna (● = transmitting antenna at ceiling, O = transmitting antenna at headrest level) and volunteers (□) within (a) the empty, (b) the partially filled and (c) the completely filled Boeing 737-200 aircraft.

III. EFFECT OF HUMAN PRESENCE ON PATH GAIN IN THE AIRCRAFT ENVIRONMENT

The manner in which path gain decreases with distance determines the maximum range that can be achieved by a wireless link. For UWB-based wireless systems, path gain is an especially important consideration given the relatively low power levels that such systems are permitted to radiate. Within the passenger cabin, path gain decreases with increasing transmitter-receiver separation due to the combined effects of spatial spreading and obstruction by cabin fixtures, seating and passengers. Assessing the effect of human presence on path gain within the aircraft environment allows system designers to more accurately predict the coverage and reliability of UWB-based point-to-multipoint wireless systems deployed within such environments.

We modeled the path gain within the passenger cabin environment as follows. First, we divided the 3.1-6.1 GHz frequency range into two band groups $b = \{1, 2\}$, each of which is 1.5 GHz wide. Over each band group, we verified that the envelope of the frequency response was effectively flat. We obtained the distance-dependent path gain $G_p(d)$ by taking the average of the magnitude of the measured complex CFRs, $H(f, d)$, across each band group, yielding

$$G_p(d) = \frac{1}{M}\sum_{i=0}^{M-1}\left|H(f_i, d)\right|^2 . \quad (1)$$

where d is the transmitter-receiver separation distance, M is the number of frequency steps in each band group, and f_i is the ith frequency step. At each location, we estimated the path gain when the cabin was empty, and then estimated the *reduction* in path gain, ΔG_p, when the cabin was partially and fully occupied. The configuration of the transmitting and receiving antennas and their antenna patterns remained constant as the level of occupancy increased. Thus, any variation in antenna gain due to changes in the path geometry

with distance would have cancelled out when the difference in the estimated path gains was calculated.

In Fig. 3, the reduction in path gain, ΔG_p, observed in band group 1 is presented as a function of distance, d, for different path types and, within each plot, for different levels of occupancy. Although we had anticipated that the reduction in path gain would generally increase with distance over the length of the cabin, the actual relationship was more complicated. Initially, path gain decreases as the distance between the transmitter and receiver increases. Beyond the mid-point in the cabin (a distance of between 7 and 9 meters), however, the trend reverses. The time dispersion results presented in the next section do not reveal a similar breakpoint at the mid-point of the cabin so it seems likely that AoA effects are responsible. Although our measurement data are insufficient to reveal such effects, ray tracing simulations similar to those described in [23] and [24] may provide additional insight and be a useful next step.

In all cases and both band groups, we found that the reduction in path gain associated with human presence was well-approximated by a quadratic expression in distance of the form

$$\Delta G_p(d) = \Delta G_{p0} + Ad + Bd^2 + X_\sigma . \qquad (2)$$

where ΔG_p , A and B are constants and X_σ is a zero-mean Gaussian random variable with a standard deviation of σ that accounts for location variability. In each case, we determined the constants ΔG_p, A and B by applying regression analysis to the measured data. We estimated σ by subtracting the quadratic regression line from the measured values of ΔG_p and fitting the results to a Gaussian distribution. The values of the parameters in each case are presented in Table I. In the C-to-H configuration, the maximum decrease in mean path gain due to human presence is relatively low (no more than a few dB), as one might expect given that the C-to-H paths are relatively unobstructed by human presence. In the C-to-A and H-to-A configurations, the maximum decrease in mean path gain is much greater (up to 10 dB), as one might expect given that the C-to-A and C-to-H paths are much more obstructed by passengers.

IV. EFFECT OF HUMAN PRESENCE ON TIME DISPERSION IN THE AIRCRAFT ENVIRONMENT

Our first step in characterizing time dispersion within the cabin was to convert the CFRs that we measured into CIRs. Following [27], we truncated the CFRs into band groups and zero-padded them to restore the original length and thus preserve the temporal resolution. If $f_{b,u}$ and $f_{b,l}$ are the upper and lower frequency boundaries of band group b, respectively, then the complex CFR for band group b is given by

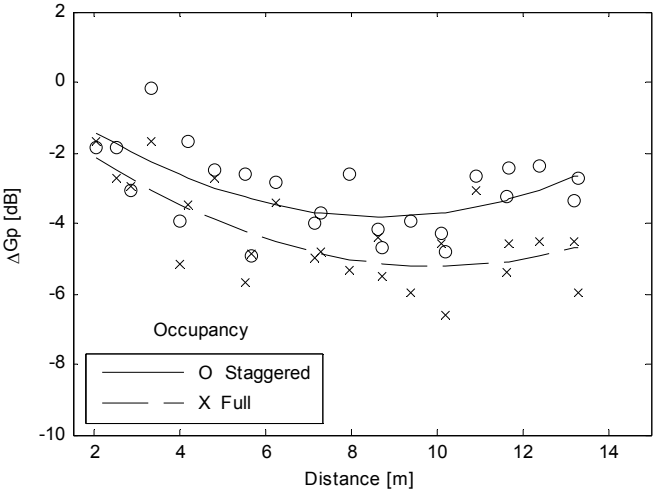

(a)

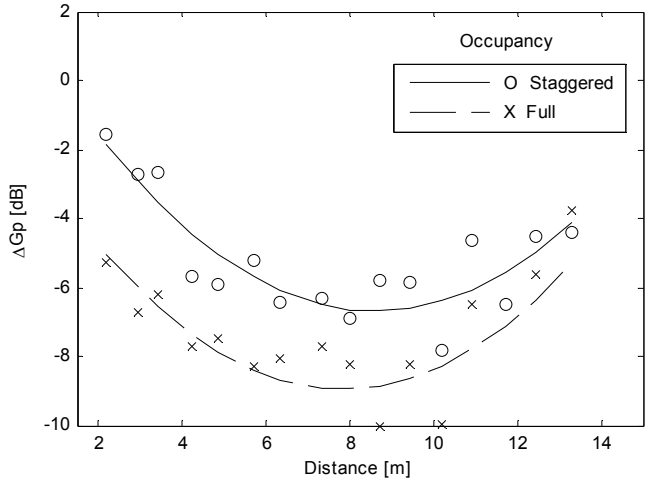

(b)

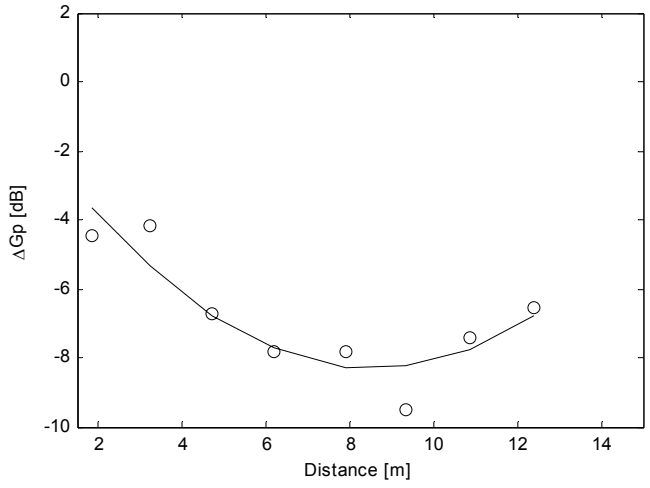

(c)

Fig. 3. Reduction in path gain with respect to distance for band group 1 for (a) ceiling-to-headrest, (b) ceiling-to-armrest, and (c) headrest-to-armrest configurations.

TABLE I
LARGE-SCALE PATH GAIN PARAMETERS FOR THE AIRCRAFT PASSENGER CABIN ENVIRONMENT

Path Type	Occupancy	Band	ΔG_{p0} [dB]	A [dB/m]	B [dB/m^2]	Location variability, σ [dB]
C-to-H	Empty	1	–	–	–	–
		2	–	–	–	–
	Staggered	1	0.261	-0.941	0.054	0.903
		2	0.718	-0.865	0.051	1.121
	Full	1	-0.326	-0.979	0.049	0.884
		2	-1.109	-0.588	0.033	1.424
C-to-A	Empty	1	–	–	–	–
		2	–	–	–	–
	Staggered	1	2.061	-2.029	0.118	0.824
		2	-0.742	-1.178	0.076	0.578
	Full	1	-1.388	-1.928	0.123	1.252
		2	-1.936	-1.582	0.105	0.881
H-to-A	Empty	1	–	–	–	–
		2	–	–	–	–
	Full	1	-0.635	-1.790	0.104	0.759
		2	1.993	-2.323	0.142	0.521

Note: C = Ceiling, H = Headrest, A = Armrest

TABLE II
LARGE-SCALE DELAY SPREAD PARAMETERS FOR THE AIRCRAFT PASSENGER CABIN ENVIRONMENT

Path Type	Occupancy	Band	Intercept, τ_i [ns]	Distance exponent (rms delay spread), γ	Residual, σ_τ [ns]	Decay time constant, τ_0 [ns]
C-to-H	Empty	1	8.21	2.12	3.65	-32.7
		2	5.72	1.88	3.66	-26.7
	Staggered	1	9.52	0.66	2.23	-19.0
		2	7.76	0.58	2.58	-18.5
	Full	1	8.46	0.76	2.58	-17.5
		2	8.05	0.43	2.70	-17.8
C-to-A	Empty	1	11.6	2.10	1.20	-37.0
		2	11.1	1.93	2.20	-37.1
	Staggered	1	10.9	0.78	1.37	-19.3
		2	14.3	0.35	1.96	-17.7
	Full	1	14.2	0.21	1.70	-18.4
		2	10.6	0.63	2.14	-16.6
H-to-A	Empty	1	14.6	1.82	0.89	-33.8
		2	13.1	1.91	0.88	-32.1
	Full	1	9.73	0.92	1.74	-17.4
		2	11.5	0.52	1.05	-18.8

$$H_b(f,d) = \begin{cases} H(f,d), & \text{if } f_{b,l} \le f \le f_{b,h} \\ 0, & \text{otherwise.} \end{cases} \quad (3)$$

Following the approach described in [31], we applied a Kaiser window with $\beta = 7$ to the CFR in order to suppress dispersion of energy between delay bins. We then applied an inverse Fourier transform (IFT) directly to the complex baseband of the CFR to yield a CIR. We expressed the result in the form of a power delay profile (PDP),

$$P_{h,b}(\tau_k) = \left|h_b(\tau_k)\right|^2 = \sum_k a_k \delta(\tau - \tau_k). \quad (4)$$

where a_k are the amplitudes (expressed in units of power) of MPCs at different delays τ_k.

Measured PDPs typical of the C-to-A configuration under empty, partially filled and completely filled conditions in the aircraft are given in Fig. 4. It is immediately apparent that the passenger cabin is rich with scatterers leading to a high density of MPCs in the PDPs. For LOS channels, we define the start of the PDP as the first MPC that arrives within 10 dB of, and 10 ns, before the peak MPC. For NLOS channels, we define the start of the PDP as the first MPC that arrives within 10 dB of, and 50 ns, before the peak MPC. We remove the propagation delay by setting the start time of the first arriving MPC to zero. These criteria are based upon those adopted by IEEE 802.15.4a and used in [32].

Using regression techniques, we estimated the decay time constants, τ_0, *i.e.*, the reciprocal of the slope of *the scattered components* in the PDPs, for various path types, degrees of occupancy and band groups. The values are given in Table II. As the density of occupancy increased from empty to half full, the decay rate of the scattered components in the PDP almost doubled. Further increases in the density of occupancy had little effect, however.

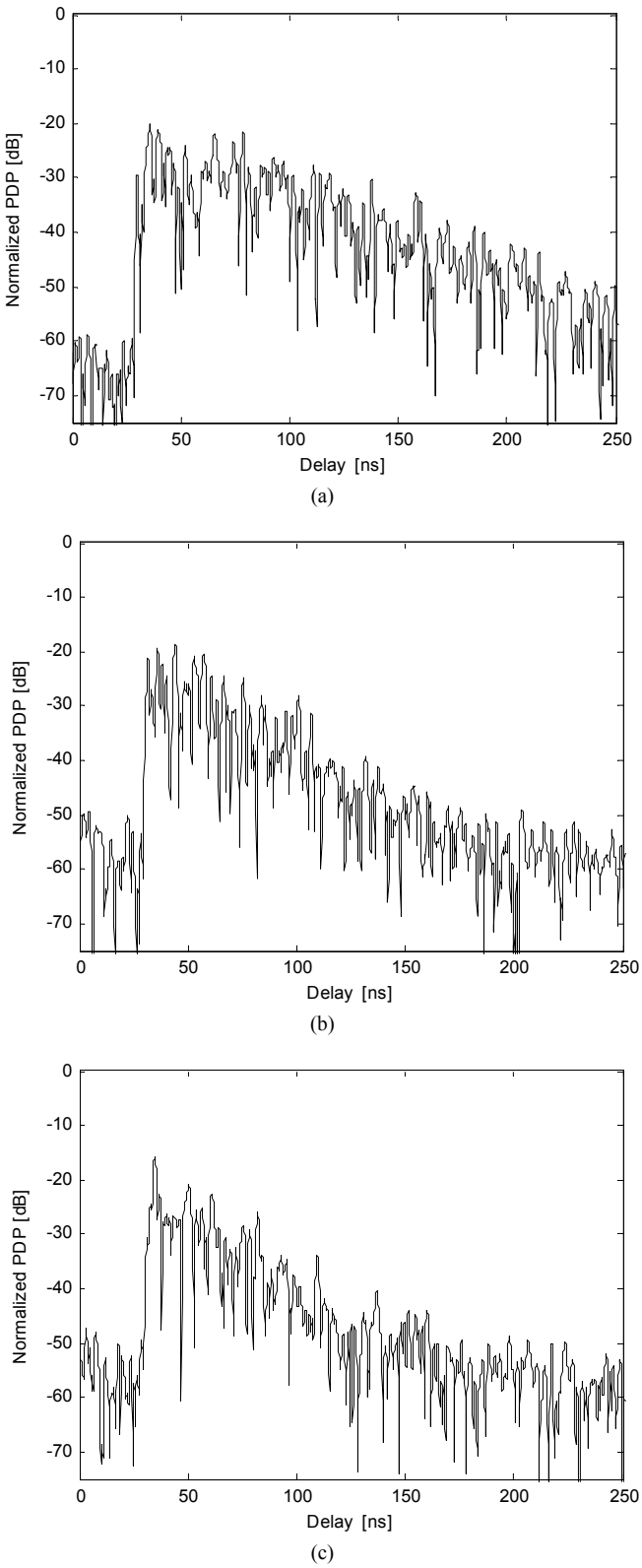

Fig. 4. The normalized power delay profiles for band group 2 for the ceiling-to-armrest path type that were observed at row 13 for occupancy levels of: (a) empty, (b) partially full, and (c) completely full.

A. Delay Spread

The normalized first-order moment of a PDP gives the mean excess delay,

$$\tau_{mean} = \frac{\sum_k P_{h,b}(\tau_k)\tau_k}{\sum_k P_{h,b}(\tau_k)}, \tag{5}$$

while the square root of the second central moment of a PDP gives the rms delay spread,

$$\tau_{rms} = \sqrt{\tau_{mean}^2 - (\tau_{mean})^2}, \tag{6}$$

where

$$\tau_{mean}^2 = \frac{\sum_k P_{h,b}(\tau_k)\tau_k^2}{\sum_k P_{h,b}(\tau_k)}, \tag{7}$$

Before we estimated the rms delay spread, we removed all MPCs with amplitudes that are more than 25 dB below the peak scattered component.

In Fig. 5, we show how rms delay spread depends upon the transmitter-receiver separation distance d for the three different path types (C-to-H, C-to-A, H-to-A) in band group 2. We model the distance dependence as

$$\tau_{rms} = \tau_i + 10\gamma \log_{10} d + X_{\sigma_\tau}, \tag{8}$$

where τ_i is the mean rms delay spread at d = 1 m, γ is the distance exponent, and X_{σ_τ} is a zero-mean Gaussian random variable with a standard deviation of σ_τ that accounts for location variability. The values of these parameters for various path types, degrees of occupancy and both band groups are given in Table II. In all cases where the aircraft was empty, the rms delay spread increased rapidly with distance while increasing the density of occupancy to half-full generally caused γ to decrease by a factor of nearly four. Increasing the density of occupancy caused little further reduction in γ. The decrease in γ is likely the result of energy in the scattered components being blocked or attenuated as the number of passengers aboard the aircraft increase.

The rms delay spread generally decreases with increasing center frequency, which is likely a consequence of the corresponding increase in attenuation and diffraction losses with frequency. Although increasing from band group 1 to 2 for the C-to-H path type causes the rms delay spread to drop by 15 - 20%, doing so for the C-to-A and H-to-A path types results in little if any reduction. The mean excess delay and rms delay spread that we observed for the C-to-H and C-to-A cases for band group 2 as a function of threshold levels of 5, 10, 15 and 20 dB below the strongest MPC are summarized in Table III and Table IV, respectively. When assessing the performance of practical systems, it may be more realistic to apply a dynamic noise threshold that accounts for the

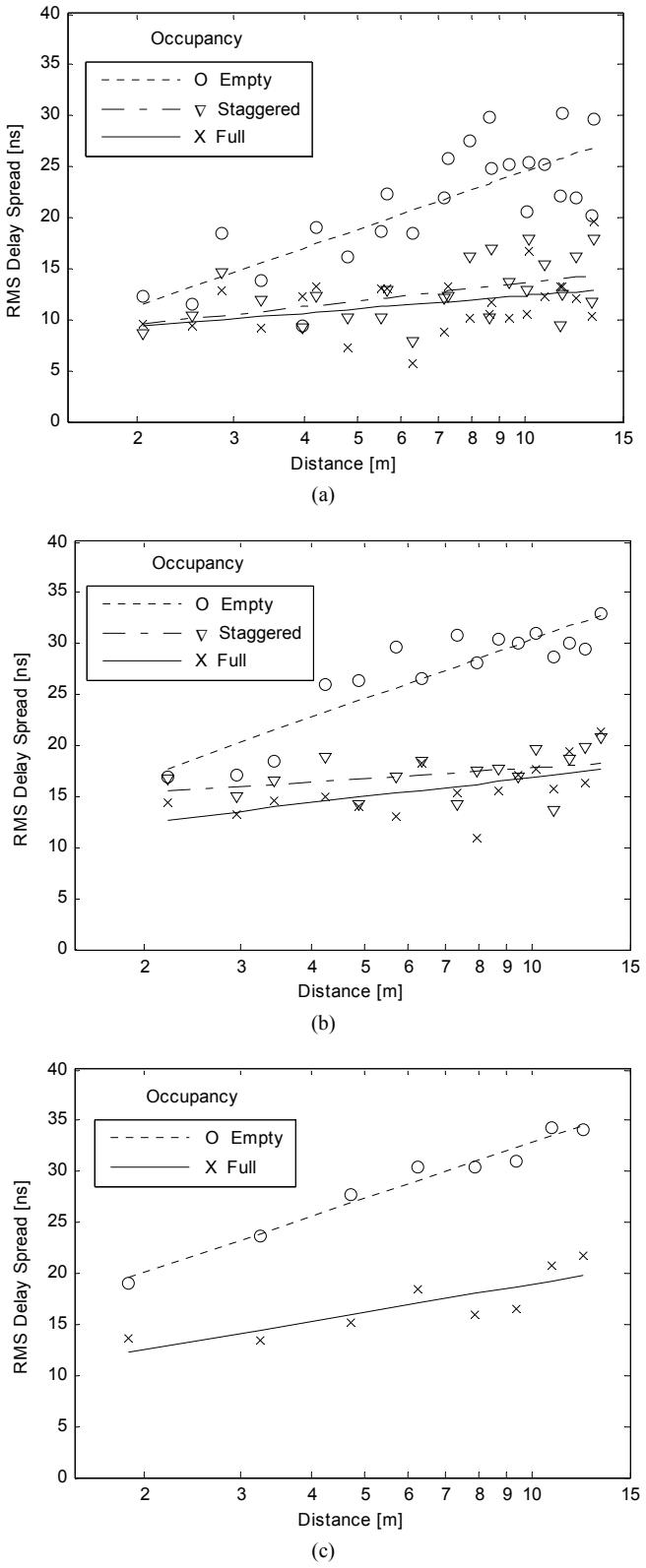

Fig. 5. RMS delay spread with respect to distance for band group 2 for (a) ceiling-to-headrest, (b) ceiling-to-armrest, and (c) headrest-to-armrest configurations.

diminishing signal-to-noise ratio and the tendency of weaker multipath components to drop below the noise floor at greater ranges.

B. Number of Significant Paths

We define a significant path as a resolvable MPC that exceeds a given threshold of 5, 10, 15 and 20 dB below the strongest MPC. In Table III and Table IV, respectively, we have summarized, as a function of the threshold level, the number of significant paths that we observed for the C-to-H and C-to-A cases and band group 2 and the percentage of energy that each set captures. We found that the PDPs associated with band group 2 have between 10 and 30% fewer significant paths at a given threshold than those associated with band group 1. Moreover, we found that the PDPs measured in a full aircraft have between 40 and 45% fewer significant paths at a given threshold than those measured in an empty aircraft. These results are consistent with our observation that the duration of the PDP shrinks with increased occupancy and increased carrier frequency.

V. CONCLUSIONS

Because the passenger cabin has a confined volume and may be densely occupied, human presence affects radiowave propagation within a midsized airliner more than in conventional indoor environments such as homes, offices and industrial sites. In order to assess the effect of human presence in such environments, we collected channel frequency response data over the range 3.1 to 6.1 GHz within the passenger cabin of a Boeing 737-200 aircraft.

Despite the essentially square layout and short extent of the widebody scenario considered in [26] compared to the compared to the long and narrow extent of the case considered here, the results obtained within the two environments showed remarkable consistency. In particular, increasing occupancy tended to increase path loss by a few dB and lower delay spread by a few tens of nanoseconds. Otherwise, the much different geometry of the two scenarios precludes meaningful detailed comparison.

Our investigation of path gain over point-to-multipoint links within the narrowbody cabin with the transmitting antenna in the front of the cabin reveals that: (1) the decrease in path gain that occurs as occupancy increases reaches a maximum near the mid-point of the cabin, decreases thereafter, and is well-approximated by a quadratic function, (2) the maximum decrease in path gain becomes more acute as: (a) the transmitting antenna drops from the ceiling to the headrest level and (b) as the receiving antenna drops from the headrest to armrest, (3) in the ceiling-to-headrest configuration, the maximum decrease in the mean path gain due to human presence is only a few dB; in the ceiling-to-armrest or headrest-to-armrest cases, the maximum decrease in the mean path gain is up to 10 dB. Although our measurement data are insufficient to reveal the physical cause of the distance-dependent behaviour, numerical simulations similar to those described in [23] and [24] may provide additional insight and might be a useful next step.

TABLE III
CEILING-TO-HEADREST CONFIGURATION -
MEAN EXCESS DELAY, RMS DELAY SPREAD, NUMBER OF SIGNIFICANT PATHS
AND ENERGY CAPTURED FOR DIFFERENT THRESHOLD LEVELS

Occupancy	Band	Threshold [dB]	τ_{mean} [nsec]	τ_{rms} [nsec]	Num. of Paths	% Power
Empty	1	5	7.85	7.06	24	27
		10	14.3	12.1	116	59
		15	20.1	18.0	288	81
		20	24.3	22.5	520	93
	2	5	1.93	1.68	12	32
		10	5.43	6.41	47	52
		15	10.8	12.3	153	75
		20	15.2	17.2	337	90
Staggered	1	5	3.13	2.43	15	32
		10	6.37	6.19	63	61
		15	9.78	9.84	158	82
		20	12.2	12.7	295	93
	2	5	1.64	1.40	11	38
		10	3.49	3.80	36	60
		15	6.14	7.18	105	80
		20	8.52	10.2	224	92
Full	1	5	2.29	2.53	15	35
		10	5.50	6.09	59	61
		15	8.91	9.61	154	83
		20	11.4	12.7	290	94
	2	5	1.06	0.79	10	40
		10	2.47	3.07	30	59
		15	4.83	6.16	88	78
		20	7.14	9.32	192	91

Note: C = Ceiling, H = Headrest, A = Armrest

TABLE IV
CEILING-TO-ARMREST CONFIGURATION -
MEAN EXCESS DELAY, RMS DELAY SPREAD, NUMBER OF SIGNIFICANT PATHS
AND ENERGY CAPTURED FOR DIFFERENT THRESHOLD LEVELS

Occupancy	Band	Threshold [dB]	τ_{mean} [nsec]	τ_{rms} [nsec]	Num. of Paths	% Power
Empty	1	5	16.9	11.7	53	32
		10	23.2	17.9	217	69
		15	29.0	22.8	458	89
		20	32.3	26.4	715	96
	2	5	11.9	7.88	41	32
		10	18.1	14.0	174	64
		15	23.6	19.3	366	85
		20	27.1	23.2	595	94
Staggered	1	5	7.85	5.34	32	38
		10	10.8	8.30	112	69
		15	14.2	12.3	246	88
		20	16.4	14.9	402	96
	2	5	5.44	3.38	24	35
		10	9.03	7.84	92	66
		15	12.4	11.3	209	86
		20	14.8	14.3	365	95
Full	1	5	6.25	4.30	29	36
		10	10.1	8.44	110	70
		15	13.0	11.3	226	88
		20	14.9	13.8	371	95
	2	5	5.12	3.42	25	37
		10	8.60	7.29	93	68
		15	11.6	10.5	208	87
		20	13.6	12.9	345	95

Our investigation of time dispersion within the narrowbody cabin reveals that: (1) the channel impulse response always presents a dense single cluster regardless of the level of occupancy, (2) the rms delay spread generally increases with distance when the aircraft is empty but is essentially uniform when the aircraft is partially or fully occupied, (3) both the rms delay spread and the number of significant paths reduces by up to half as the level of occupancy increases from empty

to half occupied, and (4) increasing the level of occupancy from half to full has little additional effect.

In summary, our results: (1) suggest that human presence substantially affects radiowave propagation within an aircraft passenger cabin and should be considered when characterizing the performance of in-cabin wireless systems and (2) will be helpful to those wishing to validate the results of software simulations of in-cabin wireless propagation. Further measurements in different aircraft will be required to assess how seatbacks that incorporate in-flight entertainment units contribute to excess shadowing on ceiling-to-armrest and headrest-to-armrest links.

ACKNOWLEDGMENT

The authors would like to thank Associate Dean Jack Baryluk, Chief Instructor/Hangar Supervisor Grant Johnson and ATC Chair Lusia Kurk of the BCIT Aerospace Technology Campus at Vancouver International Airport for providing us with access to their Boeing 737-200 aircraft and their outstanding cooperation during the course of this study.

The authors would also like to thank Wadah Muneer, Weiwen Liu, Robert White, Faye Limbo and Johnty Wang for their assistance during the measurement sessions and the many volunteers who served as part of the propagation environment within the aircraft cabin.

REFERENCES

[1] M. Ghaddar, L. Talbi and T. A. Denidni, "Human body modeling for prediction of effect of people on indoor propagation channel," *Electron. Lett*., vol. 40, no. 25, pp. 1592-1594, 9 Dec. 2004.

[2] M. Ghaddar, L. Talbi, T. A. Denidni and A. Sebak, "A conducting cylinder for modeling human body presence in indoor propagation channel," *IEEE Trans. Antennas Propag.,* vol. 55, no. 11, pp. 3099-3103, Nov. 2007.

[3] R. Ganesh and K. Pahlavan, "Effects of traffic and local movements on multipath characteristics of an indoor radio channel," *Electron. Lett*., vol. 26, no. 12, pp. 810- 812, 7 Jun. 1990.

[4] K. I. Ziri-Castro, W. G. Scanlon, and N. E. Evans, "Prediction of variation in MIMO channel capacity for the populated indoor environemnt using a radar cross-section-based pedestrian model," *IEEE Trans. Wireless Commun.*, vol. 4, no. 3, pp. 1186–1194, May 2005.

[5] K. I. Ziri-Castro, N. E. Evans and W. G. Scanlon, "Propagation modeling and measurements in a populated indoor environment at 5.2 GHz," in *Proc. AusWireless 2006*, 13-16 Mar. 2006, pp. 1-8.

[6] S. L. Cotton and W. G. Scanlon, "Characterization and modeling of the indoor radio channel at 868 MHz for a mobile bodyworn wireless personal area network," *IEEE Antennas Wireless Propag. Lett.*, vol. 6, pp. 51-55, Dec. 2007.

[7] T. B. Welch *et al*., "The effects of the human body on UWB signal propagation in an indoor environment," *IEEE J. Sel. Areas Commun.*, vol. 20, no. 9, pp. 1778-1782, Dec. 2002.

[8] A. Kara, "Human body shadowing variability in short range indoor radio links at 3-11 GHz," *Int. J. Elec.,* vol. 96, no.2, pp. 205-211, Feb. 2009.

[9] J. Karedal, A. J. Johansson, F. Tufvesson and A. F. Molisch, "Shadowing effects in MIMO channels for personal area networks," in *Proc. IEEE VTC 2006 Fall*, 25-28 Sep. 2006, pp. 1-5.

[10] A. Fort, J. Ryckaert, C. Desset, P. De Donecker, P. Wambacq and L. Van Biesen, "Ultra-wideband channel model for communication around the human body," *IEEE J. Sel. Areas Commun.*, vol. 24, no. 4, pp. 927-933, Apr. 2006.

[11] S. L. Cotton and W. G. Scanlon, "A statistical analysis of indoor multipath fading for a narrowband wireless body area network," in *Proc. IEEE PIMRC'06*, Sep. 2006, pp. 1-5.

[12] A. Alomainy, Y. Hao, A. Owaldally, C. G. Parini, Y. I. Nechayev, and C. C. Coonstantinou and P. S. Hall, "Statistical analysis and performance evaluation for on-body radio propagation with microstrip patch antennas," *IEEE Trans. Antennas Propag.,* vol. 55, no. 1, pp. 245-248, Jan. 2007.

[13] N. R. Diaz and M. Holzbock, "Aircraft cabin propagation for multimedia communications," in *Proc. EMPS 2002*, 25-26 Sep. 2002, pp. 281-288.

[14] A. Jahn *et al*., "Evolution of aeronautical communications for personal and multimedia services," *IEEE Commun. Mag.*, vol. 41, no. 7, pp. 36-43, Jul. 2003.

[15] N. R. Diaz and J. E. J. Esquitino, "Wideband channel characterization for wireless communications inside a short haul aircraft," in *Proc. IEEE VTC 2004 - Spring*, 17-19 May 2004, pp. 223-228.

[16] R. Bhagavatula, R. W. Heath and S. Vishwanath, "Optimizing MIMO antenna placement and array configuration for multimedia delivery in aircraft," in *Proc. IEEE VTC 2007 Spring*, 22-25 Apr. 2007, pp. 425-429.

[17] A. Kaouris, M. Zaras, M. Revithi, N. Moraitis and P. Constantinou, "Propagation measurements inside a B737 aircraft for in-cabin wireless networks," in *Proc. IEEE VTC 2008 Spring*, 11-14 May 2008, pp. 2932-2936.

[18] A. F. Molisch, J. R. Foerster and M. Pendergrass, "Channel models for ultrawideband personal area networks," *IEEE Wireless Commun.*, vol. 10, no. 6, pp. 14-21, Dec. 2003.

[19] A. F. Molisch *et al.,* "A comprehensive standardized model for ultrawideband propagation channels," *IEEE Trans. Antennas Propag.,* vol. 54, no. 11, pp. 3151-3165, Nov. 2006.

[20] J. Chuang, N. Xin, H. Huang, S. Chiu and D. G. Michelson, "UWB radiowave propagation within the passenger cabin of a Boeing 737-200 Aircraft," in *Proc. IEEE VTC 2007 Spring*, 22-25 Apr. 2007, pp. 496-500.

[21] J. Jemai *et al*., "UWB channel modeling within an aircraft cabin," in *Proc. IEEE ICUWB 2008*, 10-12 Sep. 2008, pp. 5-8.

[22] G. A. Breit, H. Hachem, J. Forrester, P. Guckian, K. P. Kirchoff and B. J. Donham, "RF propagation characteristics of in-cabin CDMA mobile phone networks," in *Proc. Digital Avionics Syst. Conf. 2005*, 30 Oct.-3 Nov. 2005, pp. 9.C.5-1--9.C.5-12.

[23] M. Youssef and L. Vahala, "Effects of passengers and internal components on electromagnetic propagation prediction inside Boeing aircrafts," in *2006 IEEE AP-S Int. Symp. Dig.*, 9-14 Jul. 2006, pp. 2161-2164.

[24] T. Hikage, T. Nojima, M. Omiya and K. Yamamoto, "Numerical analysis of electromagnetic field distributions in a typical aircraft," in *Proc. EMC Europe 2008*, 8-12 Sep. 2008, pp. 1-4.

[25] M. P. Robinson, J. Clegg and A. C. Marvin, "Radio frequency electromagnetic fields in large conducting enclosures: effects of apertures and human bodies on propagation and field-statistics," *IEEE Trans. Electromagn. Compat.*, vol. 48, no. 2, pp. 304-310, May 2006.

[26] M. Jacob et al., "Influence of passengers on the UWB propagation channel within a large wide-bodied aircraft," in *Proc. EuCAP 2009*, 23-27 Mar. 2009, pp. 882-886.

[27] ECMA International, "High rate – ultra wide band (UWB) background," Available: www.ecma-international.org/activities/communicaitons/tg20_UWB_Background.pdf

[28] A. F. Molisch, "Ultrawideband propagation channels: Theory, measurement, and modeling", *IEEE Trans. Veh. Technol.,* vol. 54, no.5, pp. 1528–1545, Sep. 2005.

[29] J. Wang, A. S. Mohan and T. A. Aubrey, "Angles-of-arrival of multipath signals in indoor environments," in *Proc. IEEE VTC 1996*, 28 Apr. – 1 May 1996, pp. 155-159.

[30] W. Q. Malik, D. J. Edwards and C. J. Stevens, "Frequency dependence of fading statistics for ultrawideband systems," *IEEE Trans. Wireless Commun.*, vol. 6, no. 3, pp. 800-804, Mar. 2007.

[31] S. S. Ghassemzadeh, R. Jana, C. W. Rice, W. Turin and V. Tarokh, "Measurement and modeling of an ultra-wide bandwidth indoor channel," *IEEE Trans. Wireless Commun*., vol. 52, no. 10, pp. 1786-1796, Oct. 2004.

[32] C. C. Chong and S. K. Yong, "A generic statistical-based UWB channel model for high-rise apartments," *IEEE Trans. Antennas Propag.*, vol. 53, no. 8, pp. 2389-2399, Aug. 2005.

[33] V. Erceg *et al*., "A model for the multipath delay profile of fixed wireless channels," *IEEE J. Sel. Areas Commun.,* vol. 17, no. 3, pp. 399-410, Mar. 1999.

Simon Chiu was born in Hong Kong, China in 1984. He received the BASc and MASc degrees in Electrical Engineering from the University of British Columbia, Vancouver, BC, Canada in 2006 and 2009, respectively.

His main research interests focus on UWB propagation in passenger aircraft cabins and outdoor industrial environments as well as the effects of human presence.

David G. Michelson (S'80-M'89-SM'99) received the B.A.Sc., M.A.Sc., and Ph.D. degrees in Electrical Engineering from the University of British Columbia (UBC), Vancouver, BC, Canada.

From 1996 to 2001, he served as a member of a joint team from AT&T Wireless Services, Redmond, WA, and AT&T Labs-Research, Red Bank, NJ, where he was concerned with the development of propagation and channel models for next-generation and fixed wireless systems. The results of this work formed the basis for the propagation and channel models later adopted by the IEEE 802.16 Working Group on Broadband Fixed Wireless Access Standards. From 2001 to 2002, he helped to oversee the deployment of one of the world's largest campus wireless local area networks at UBC while also serving as an Adjunct Professor with the Department of Electrical and Computer Engineering. Since 2003, he has led the Radio Science Laboratory, Department of Electrical and Computer Engineering, UBC, where his current research interests include propagation and channel modeling for fixed wireless, ultra wideband, and satellite communications.

Prof. Michelson is a registered professional engineer. He serves as the Chair of the IEEE Vehicular Technology Society Technical Committee on Propagation and Channel Modeling and as an Associate Editor for Mobile Channels for IEEE Vehicular Technology Magazine. In 2002, he served as a Guest Editor for a pair of Special Issues of the IEEE JOURNAL ON SELECTED AREAS IN COMMUNICATIONS concerning propagation and channel modeling. From 2001 to 2007, he served as an Associate Editor for the IEEE TRANSACTIONS ON VEHICULAR TECHNOLOGY. From 1999 to 2007, he was the Chair of the IEEE Vancouver Section's Joint Communications Chapter. Under his leadership, the chapter received Outstanding Achievement Awards from the IEEE Communications Society in 2002 and 2005 and the Chapter of the Year Award from IEEE Vehicular Technology Society in 2006. He received the E. F. Glass Award from IEEE Canada in 2009 and currently serves as Chair of IEEE Vancouver Section.